The Use and Refinement of Neutron Imaging Techniques for Archaeological Artifacts

Krysta Ryzewski, Hassina Z. Bilheux, Susan N. Herringer, Jean-Christophe Bilheux, Lakeisha Walker, and Brian W. Sheldon

Neutron imaging is a noninvasive, nondestructive technique that generates data about the structure, properties, and composition of materials in two and three dimensions (i.e., radiography and computed tomography) (Lehmann and Pleinert 1998; Schillinger 1996). Most archaeological artifacts may be mapped with neutron imaging, including those crafted with metals and hydrogen-rich organic materials whose properties and constituents are not easily discerned from other imaging techniques. Neutron imaging is not limited in scope to microscopic objects or partial samples of larger artifacts. Any objects whose dimensions fall within the instrument's range of transmission and contrast can be imaged.

Neutron imaging is becoming an exceptionally valuable tool for archaeological researchers because it is a cost-effective, nondestructive technique. Neutron imaging instruments quickly produce comprehensive visual, quantitative, and qualitative data about objects, materials, or residues at a variety of scales (from tens of microns to macro-scale). The two- and three-dimensional visual, compositional, and structural data produced by the imaging process enriches, and in some cases substantiates, a multitude of archaeological research avenues. These include the examination of entire fragile objects, systematic evaluation of material performance over time, identification and analysis of past manufacturing techniques, and determination of object

ABSTRACT

Neutron imaging is a nondestructive application capable of producing two- and three-dimensional maps of archaeological objects' external and internal structure, properties, and composition. This report presents the recent development of neutron imaging data collection and processing methods at Oak Ridge National Laboratory (ORNL), which have been advanced, in part, by information gathered from the experimental imaging of 25 archaeological objects over the past three years. The dual objectives of these imaging experiments included (1) establishing the first methodological procedures for the neutron imaging of archaeomaterials involving the CG-1D beamline and (2) further illustrating the potential of neutron imaging for archaeologists to use in the reverse engineering of ancient and historical objects. Examples of objects imaged in two and three dimensions are provided to highlight the application's strengths and limitations for archaeological investigations, especially those that address ancient and historic technologies, materials science, and conservation issues.

L'imagerie avec les neutrons (ou imagerie neutronique) est une application non-destructive et capable de produire des cartes de structures externes et internes, de propriétés et composition, en 2 et 3 dimensions d'objets archéologiques. Ce rapport présente l'évolution récente de l'acquisition des images à neutrons, des méthodes de traitement d'image au Laboratoire National d'Oak Ridge (ORNL), qui ont été avancées, en partie, par des informations recueillies par les mesures expérimentales de 25 objets archéologiques au cours des trois dernières années. L'objectif double de ces expériences d'imagerie était le suivant: (1) l'établissement des premières procédures méthodologiques pour l'imagerie avec les neutrons des matériaux archéologiques sur la ligne de faisceau CG-1D et la future ligne VENUS, et (2) la démonstration du potentiel de l'imagerie neutronique pour aider les archéologues à pouvoir étudier la rétroingénierie d'objets antiques et historiques. Des exemples d'objets imagés en deux et trois-dimensions sont décrits dans cet article afin de mettre en évidence les avantages et inconvénients de l'imagerie neutronique pour les recherches archéologiques, notamment celles qui traitent des technologies antiques et historiques, la science des matériaux, et des problèmes de conservation.

https://doi.org/10.7183/2326-3768.2.2.91 Published online by Cambridge University Press

KEY TERMS

Neutron: Subatomic particle with no electric charge.

Neutron vs. X-ray interaction with matter: X-rays, a form of electromagnetic radiation, interact primarily with electrons, meaning that their interaction probability (and thus attenuation) increases with atomic number. Neutrons, which have no charge, interact with atomic nuclei and do not behave according to a strict correlation between atomic number and attenuation. Neutrons can, therefore, penetrate greater thicknesses of metal than X-rays.

Attenuation: Attenuation of the incident neutron beam is the loss of radiation as it passes through a medium. A neutron beam is attenuated by scattering and absorption of the neutrons by the sample. Each element has a distinct attenuation coefficient, which is dependent on the energy distribution of the incident beam.

Neutron imaging types: In (2D) neutron radiography, a neutron beam passes through a sample of a certain thickness. A detection system measures the distribution of intensity that passes through the sample, giving a two-dimensional map of attenuation integrated along the beam path. In other words, through thickness, attenuation distribution is not obtained. In neutron tomography, intensity distributions (radiographs) are measured from equally spaced rotational intervals. The sample volume is reconstructed and gives a volumetric distribution of sample attenuation.

Beamline: A path for radiation to travel from a large-scale source (e.g., a research reactor such as HFIR) to an experimental station, typically through various filters to give the desired properties for a given type of material investigation.

Neutron diffraction: A measurement technique utilizing the elastic neutron scattering behavior of a given material in order to determine its structure.

stability and preservation, especially in relation to planning appropriate conservation treatments.

Since 2011, as part of an experimental and instrument development-based initiative, the authors have collected and processed three-dimensional neutron imaging data on more than two dozen archaeological objects of various sizes, ages, and materials using the CG-1D beamline at the High Flux Isotope Reactor (HFIR) at Oak Ridge National Laboratory (ORNL) in Tennessee, USA. This report presents an overview of recent developments in neutron imaging techniques that have occurred alongside the examination of archaeological objects at ORNL over the past three years. The discussion outlines the process of neutron imaging with the CG-1D instrument at ORNL with specific attention to the application's strengths and limitations for archaeological research purposes. Two case studies—a bronze earring from Petra, Jordan, and a bronze Roman-period dog figurine—illustrate the data collection and analytical processes involved in the imaging technique's development. The objects' imaging results convey the challenges of conducting neutron imaging on archaeological materials, but also highlight the potential benefits of the technique for archaeologists and other scholars who investigate ancient or historic technologies, materials science, and conservation issues. Three-dimensional neutron imaging is not a new technique worldwide, but due to the limited availability of suitably powerful neutron sources in the United States, these experiments are among the first of their kind performed in North America.

NEUTRON IMAGING AND ARCHAEOLOGICAL RESEARCH

Over the past two decades, pioneering studies emerging primarily from European nuclear facilities (e.g., ISIS and PSI) have illustrated both the application of neutron radiography and tomography to cultural heritage-based research and the complementary aspects of neutron and X-ray data in the analysis of archaeological objects (Anderson et al. 2009; Andreani et al. 2009; Lang and Middleton 2005; Lehmann 2006, 2009; Peetermans et al. 2012; Penumadu 2009; Schillinger 1996; Shatokha et al. 2009; Tout et al. 1980). Two-dimensional radiography has been employed to evaluate the construction techniques and materials of Roman-period weaponry and armor (Deschler-Erb et al. 2004). Three-dimensional computed tomography, using neutron attenuation coefficients, has successfully detailed the manufacturing structure and core material in bronze sculptures of the Roman god Mars and Tibetan Buddha (Festa et al. 2008; Lehmann, Deschler-Erb, and Ford 2010; Lehmann, Hartmann, and Speidel 2010; van Langh et al. 2009). Additionally, three-dimensional imaging has been coupled with neutron diffraction to map the composition and corrosion phase distribution within Etruscan Villanovan-age and Renaissance bronze statues (Festa et al. 2008; van Langh et al. 2011). Although the majority of archaeological imaging studies to date have focused on bronzes, researchers have also applied neutron imaging to glass, ceramics, and other metal artifacts to address questions of construction and composition (Fiori et al. 2006) and to inform conservation treatments (Prudêncio et al. 2012).

Most recently, owing to the increased availability and implementation of digital detection systems (i.e., charge-coupled devices or CCDs), improvements in beam quality and intensity, and increasing spatial resolution, new developments have been made with the ability to produce high-fidelity tomographic maps of archaeological materials (Andreani et al. 2009; de Beer et al. 2009; Kardjilov et al. 2012; Lehmann, Deschler-Erb, and Ford 2010; Lehmann, Hartmann, and Speidel 2010; Ryzewski et al. 2013). The authors' experiments with the CG-1D beamline at ORNL are one example of these current advances towards the multi-method and multidimensional mapping of archaeological materials.

INSTRUMENTATION AT OAK RIDGE NATIONAL LABORATORY

First commissioned in 2010, the CG-1D neutron imaging prototype beamline is located in the Cold Guide Hall of the HFIR at ORNL. The beamline provides cold neutrons between .8 and 6 Å with no wavelength discrimination (i.e., white beam mode). Figure 1 illustrates the basic design and process of the CG-1D neutron imaging beamline.

https://doi.org/10.7183/2326-3768.2.2.91 Published online by Cambridge University Press

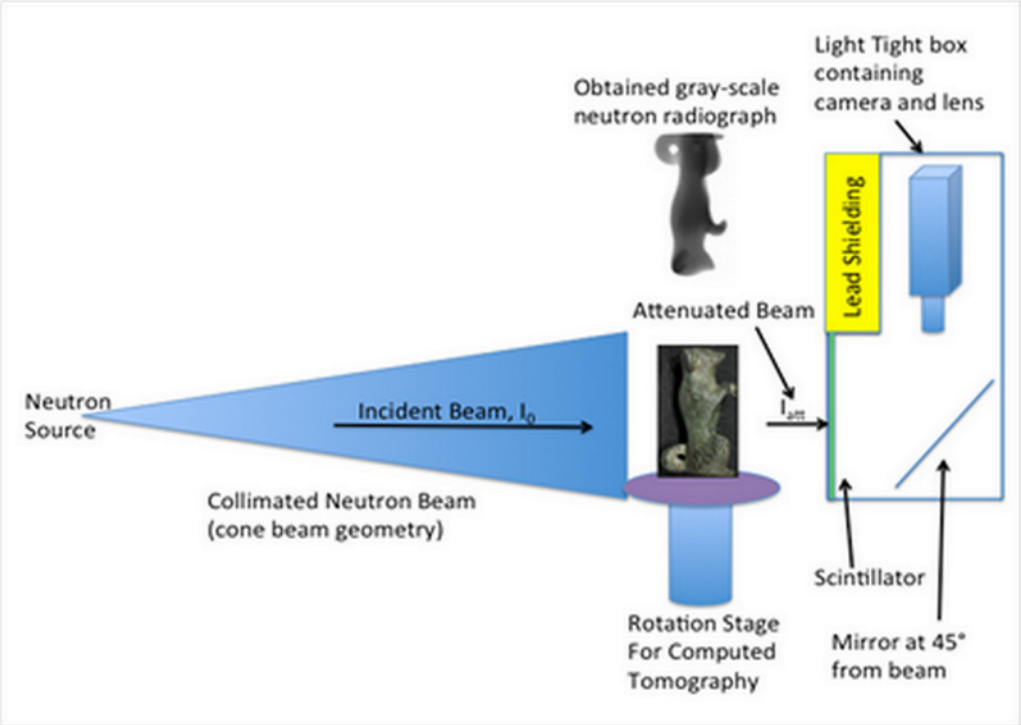


FIGURE 1. Basic layout of a neutron imaging beamline showing the neutron beam, the sample positioned on a rotation stage, and the detector system (scintillator combined charge-coupled device or CCD camera and lens).

CG-1D acquires radiographs using a DW936 ANDOR™ CCD camera that produces 16-bit digital images (Figure 2). Four inches of lead shielding is placed between the sample and the CCD in order to minimize the interaction of gammas (mainly coming from the sample) with the camera. The current flux at CG-1D (with a 12 mm aperture) is 7.5 x 10^7 n/cm^2/s. Currently the CG-1D beamline is capable of producing two and three- dimensional neutron images with a field of view (FOV) of ~ 7 x 7 cm^2 and a spatial resolution of ~ 50–75 µm. At the highest resolution, the FOV imposes limits on the area of the sample that can be imaged with one scan. However, the CG-1D is equipped with a beamline that is much larger than the FOV, permitting users to image objects with dimensions greater than 7 x 7 cm^2. Imaging larger samples requires either increasing the distance between the detector and object or conducting multiple scans across the entirety of the artifact. In the latter case, objects are reconstructed from individual scan segments during post-imaging processing.

Experimental imaging using the CG-1D is contributing to the development the instrument's operational and analytical capabilities by identifying and addressing the challenges of working with archaeological materials of various compositions, sizes, and states of preservation. The CG-1D instrument is a prototype for the Versatile Neutron Imaging Instrument (VENUS), which is currently in the planning stages at the laboratory's Spallation Neutron Source (SNS). The findings from these CG-1D experiments will be used to inform the methodological and logistical procedures for the analysis of archaeomaterials using VENUS. When online, VENUS will enable nondestructive neutron and X-ray imaging data to be gathered from large objects in two and three dimensions. VENUS will also permit the analysis of archaeological samples' material properties and structure through its ability to determine optimum wavelength range for better contrast (i.e., energy-selective and Bragg edge imaging), identify elemental compositions at specific locations within samples, map crystalline structures, and differentiate between isotopes across the entire terrain of an object (i.e., energy resonance imaging) (Anderson et al. 2009; Kardjilov et al. 2012; Sansisteban et al. 2002). Similar to the CG-1D, VENUS will be capable of collecting three-dimensional (i.e., tomographic) images of objects, though within a significantly larger 28-x-28-cm^2 fully illuminated field of view, at approximately 10–15 µm spatial resolution.

CG-1D NEUTRON IMAGING PROCEDURE

Twenty-five ancient and historical archaeological objects loaned from the collections of the Joukowsky Institute for Archaeology and the Ancient World, the Haffenreffer Museum of Anthropology at Brown University, and the Detroit Historical Museum were analyzed during multiple experimental cycles on the CG-1D beamline between August 2011 and August 2013. The majority of the objects examined (24 of 25) were metal (copper, copper alloy, iron, and silver); the last object was a ceramic. The objects were strategically selected with the dual objectives of (1) gathering comprehensive imaging data on metal artifacts of various sizes, qualities, and manufacturing techniques and (2) defining and optimizing the parameters of the CG-1D in relation to the objects' compositional and spatial variability. Two data tables summarize the properties and image acquisition protocols for the objects examined to date (Table 1 and Table 2).

https://doi.org/10.7183/2326-3768.2.2.91 Published online by Cambridge University Press

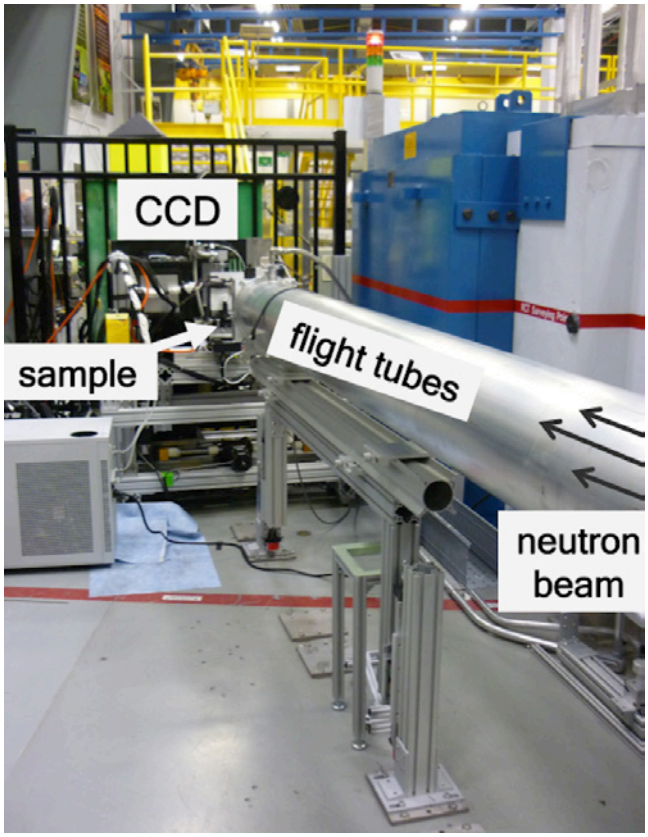


FIGURE 2. Photograph of the CG-1D imaging beamline showing the helium-filled aluminum flight tubes. Helium is used to minimize scattering of the neutrons as they travel from the source to the sample area.

Metals were chosen as the focal point of this neutron imaging study because they are among the most difficult materials to analyze using X-rays and other imaging techniques. Neutrons' advantages over X-rays result from their unique composition and behavior, which permits them to penetrate greater thickness in metals. As particles with no charge, neutrons interact with atomic nuclei and do not behave according to a strict correlation between atomic number and attenuation. In contrast, X-rays are a form of electromagnetic radiation that interact primarily with electrons; their interaction probability (and thus attenuation) increases with atomic number.

The neutron imaging procedure for the CG-1D instrument involved nine steps, most of which were completed prior to imaging (Table 3). The first step of the imaging process involved gathering information about the sample object's elemental composition. This requirement presented an acute challenge for working with this study's metal archaeological objects, whose composition was impossible to calculate accurately due to surface corrosion and internal material heterogeneity (Peetermans et al. 2012). It is not usually possible for archaeologists to identify and account for all of the unknown variables that contributed to an archaeological object's manufacture in antiquity. Therefore, the elemental compositions in this study were best approximations compiled by consulting published compositions of comparable objects and gathering compositional data from other analytical techniques (e.g., gamma spectroscopy, X-ray fluorescence).

Second, the post-imaging radioactivity of each archaeological sample was predicted by calculating the decay rate of its constituent elements in relation to the intended time of its exposure to the neutron beam. Decay rate and exposure time calculations are necessary for planning the length of the image cycle, facilitating three-dimensional virtual reconstruction, and ensuring the timely return of the samples to their home institutions according to the terms of the loan agreement (in this case, one year). In calculating the exposure lengths and decay rates, the research team consulted the beamline-specific Sample Activation Calculation (SAC), a tool developed by the ORNL Neutron Sciences Directorate (NScD). In the two- and three-dimensional imaging scenarios discussed below, the exposure time for each sample was calculated based on desired signal to noise ratio, spatial resolution, and image quality.

The SAC determined each object's exposure time and, in the case of three-dimensional imaging, the number of projections necessary for achieving the desired image resolution. The number of projections (i.e., radiograph at a given angle) were dependent on the amount of time needed to collect the projection and were limited by the predicted sample activation and corresponding decay rate. Before beginning data collection, during the third and final pre-imaging step, the object to be imaged was placed on the CG-1D platform and a series of 20- to 30-second test exposures were run to identify and adjust the position of the object within the instrument's field of view. Table 3 summarizes the remaining sequence of steps, which involve

https://doi.org/10.7183/2326-3768.2.2.91 Published online by Cambridge University Press

TABLE 1. Archaeological Objects Imaged in Two Dimensions (Radiography).

Object	Context	Dimensions (cm)	Exposure Time x Number of Scans per Object
Bronze Hanging Lamp	From Boscoreale; Late Roman, Lewis Collections, JIAAW, LC-025	20.5 (l) x 11 (h)	300 sec x 3
Bronze Standing Lamp	JIAAW Collections #276	14.5(w) x 5 (h) x 17 (l)	180 sec x 3
Bronze Coin 4	Trebonianus Gallus, 251–253 A.D., unknown provenience, Roman, JIAAW Collections, C057.08.01	.4 (w) x 2.9–3.2 (dia)	180 sec x 1
Bronze Coin 5	Hadrian, 117–138 A.D., Roman, JIAAW Collections, C042.05.02	.5 (w) x 3.2 (dia)	180 sec x 1
Bronze Coin 6	Unidentified corroded coin, Roman, JIAAW Collections. C003.04.03	.3 (w) x 2.3 (dia)	180 sec x 1
Bronze Coin 8	Hadrian, 117–138 A.D., Roman, JIAAW Collections, C042.04.04	.3 (w) x 2.5 (dia)	180 sec x 1
Brass Anklet	Boat-shaped anklet, l9th–early 20th century, ethnographic object from Senufo, Ivory Coast, Africa. Haffenreffer Museum of Anthropology Collections, 1999-22-3.	16.7 (l) x 8.2 (w) x 5.3 (h) x .59 (thickness)	12 min x 1
Brass Pipe Bowl	Tobacco pipe bowl covered with exterior overlay pattern, possibly of different alloy. Ethnographic object, Frafra, Ghana, Africa. Haffenreffer Museum of Anthropology Collections, 2012-4-6.	5.9 (w) x 5.7 (h) x .68 (thickness)	29 min 43 sec x 1

Note: Spatial Resolution between 50–100 µm.

collecting image data, monitoring data collection, safe handling of the radioactive sample, and data processing.

ARCHAEOLOGICAL OBJECTS

Eight of the 25 objects were imaged exclusively in two dimensions (Table 1). During two-dimensional imaging, each object was positioned in front of the scintillator on an unrestricted platform. Collection of two-dimensional images (i.e., radiographs) required only a few beam exposures per sample within the field of view, resulting in a significantly shorter decay period. In some cases, as with the Late Roman hanging lamp in Figure 3, the object was wider than the beamline's field of view. Such oversized objects were imaged by collecting sectional radiographs, which were later stitched together as two-dimensional photomosaics. Other factors preventing three-dimensional imaging involved objects that required measurement at a resolution or at spatial intervals that would exceed the amount of instrument time available, as well as those whose elemental composition would result in a radioactive decay time that would surpass the loan period by several years (e.g., the Ghanaian brass pipe, due to high zinc content).

Seventeen objects were mapped in three dimensions (Table 2). In preparation for three-dimensional imaging, the stage (with object secured to it) was rotated 180° in equal spatial intervals. Test images were taken during the rotation to confirm that the entire object fit within the field of view at all angles. Before beginning a full three-dimensional imaging cycle, one test exposure at the designated exposure time was run to confirm the optimization of the CCD dynamic range (i.e., optimum contrast).

During three-dimensional imaging, Data Acquisition System (DAS) computers were used to track the real-time process on the CG-1D instrument. At the end of each imaging cycle, all of the two-dimensional data were normalized using an in-house tool based on MatLab® called iMARS (Image Manipulation and Analysis Research Software). The three-dimensional projections were normalized, then reconstructed at a later time using a commercial software called Octopus (Dierick, 2005), which is based on the filtered back-projection technique. During the final and lengthiest stage, image processing, a combination of iMARS and ImageVis3D was used to perform the filtering of data, pixel identification by density and color, and the intensity measurement of data within each tomographic slice.

The process and parameters for imaging each of the 17 objects in three dimensions, including determining the number of projections, rotation step size, and exposure time, varied considerably according to the calculated run time of each experiment, estimated decay time of the objects' material constituents, and size of the object (Table 2). In three instances, multiple images were collected at the same time by attaching small objects with similar compositions (e.g., the coins and the small finds—pin, buckle, nails) to aluminum plates, each of which fit comfortably within the instrument's 7-x-7-cm^2 field of view (Figure 4). Each aluminum plate and the attached artifacts were then imaged as

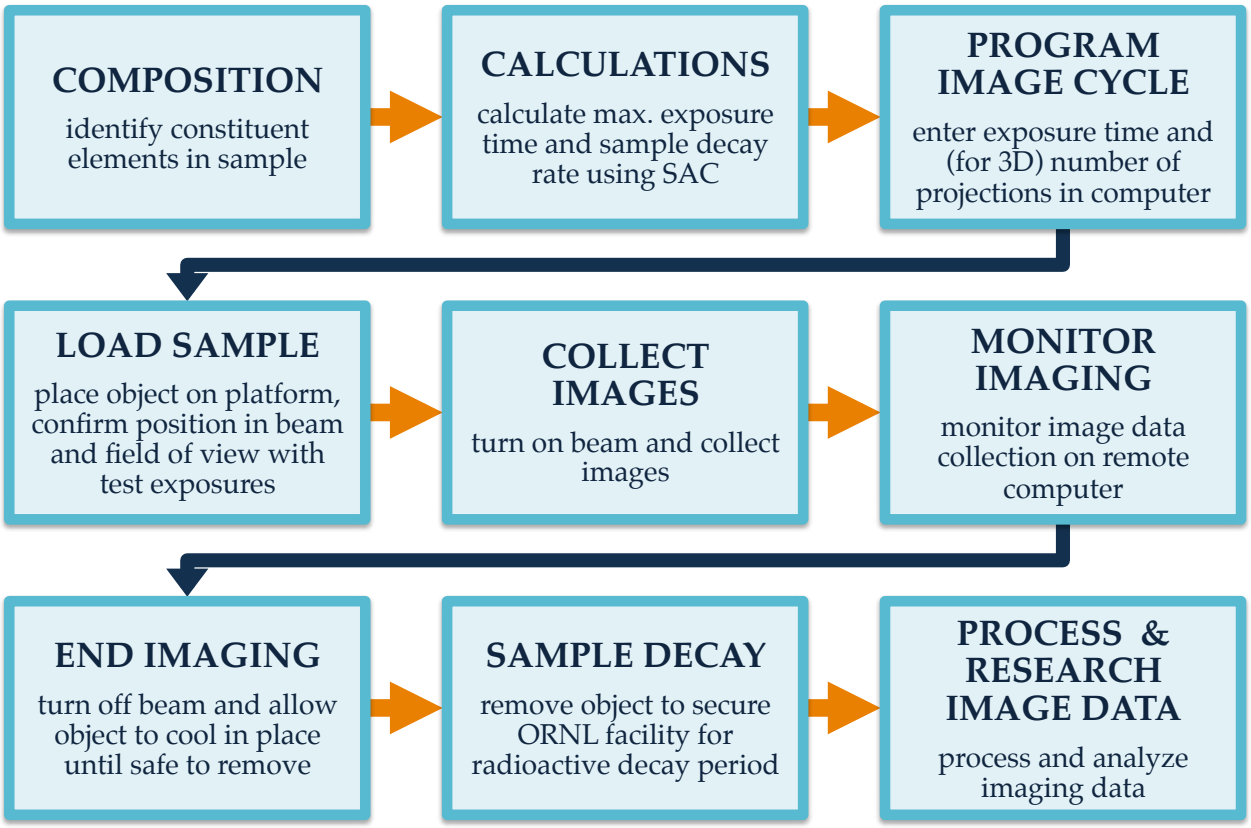
https://doi.org/10.7183/2326-3768.2.2.91 Published online by Cambridge University Press

TABLE 2. Archaeological Objects Imaged in Three Dimensions (Neutron Computed Tomography).

Object	Context	Dimensions (cm)	Exposure Time (Seconds) per Projection (Degrees)	Number of Projections	Total Image Collection Time (Hours)
Bronze Dog Figurine	Roman-period, Eastern Mediterranean region. Wagner Collection, JIAAW, JF000-04-0286, 286.	2.4 (w) x 7.5 (h)	280s per 1˚	182	14.7
Bronze Earring	Petra, Jordan. Roman, post 106 A.D. Great Temple Excavations (2001), Tr.79 Loc. 13, 79212.	3 (dia)	180s per .5˚	361	19.5
Bronze Votive Coin	Roman Style. JIAAW collections.	1.1 (max. width) 6.4 (dia)	120s per 1˚	360	13.5
Bronze Oinochoe (imaged in 2 sections)	Roman-period, JIAAW, Wagner collection, JI-0000-04-0272	8.5 (h) x 7 (w)	(top) 280s per .5˚ (bottom) 280s per .5˚	364	29.3
Bronze Coin 1	Gordianus III, 238-244 A.D., Rome mint, JIAAW collections, C055.06.03	.4 (w) x 3.0 (dia)	130s per .5˚	364	14.1
Bronze Coin 2	Gordianus III, 238–244 A.D., Rome mint, JIAAW collections, C055.06.04	.4 (w) x 3.1 (dia)	130s per .5˚	364	14.1
Bronze Coin 3	Gordianus III, 238–244 A.D., Rome mint, JIAAW collections, C044.06.05	.4 (w) x 3.5 (dia)	130s per .5˚	364	14.1
Silver Coin 7	Antoninus Pius, 138–161 A.D., JIAAW collections, C043.06.02	.2 (w) x 2.0 (dia)	180s per 1.2˚	151	8
Silver Coin 9	Hadrian, Alexandria mint(?), 117–138 A.D., JIAAW collections, C009.08.01	.4 (w) x 2.3 (dia)	180s per 1.2˚	151	8
Silver Coin 10	Antoninus Pius, 138–161 A.D., JIAAW collections, C043.05.06	.2 (w) x 2.0 (dia)	180s per 1.2˚	151	8
Ceramic Vase	Glazed and painted. Pewabic Pottery, first decade of 20th century, Detroit, MI, Detroit Historical Museum Collections	6 (h) x 6 (w) x .4 (thickness)	180s per .5˚	364	19.2
Copper Alloy Ear Spool 1	Chimu earspool, Haffenreffer Museum, Bristol, RI	4.1 (h), 5.7 (face dia), 3.56 (cylinder dia), .042 (thickness)	140s per .5˚	364	14.6
Copper Alloy Ear Spool 2	Chimu earspool, Haffenreffer Museum, Bristol, RI	4.1 (h), 5.7 (face dia), 3.56 (cylinder dia), .042 (thickness)	140s per .5˚	364	14.6
Bronze Spike Nail	Roman-period Petra, Great Temple, P.95, Loc10, 95875	6.9 (h) x .65 (w)	60s per .5˚	364	6.5
Brass Straight Pin	Greene Farm Old House site, Warwick, Rhode Island, 17th century, GF1600	4.2 (h) x .14 (thickness)	60s per .5˚	364	6.5
Brass Clothing Buckle	Greene Farm Old House site, Warwick, Rhode Island, 17th century, GF1600	2.7 (dia) x 2.9 (w) x .23 (thickness)	60s per .5˚	364	6.5
Iron Nail	Greene Farm Ironworking site, Warwick, Rhode Island, mid-late 18th century, GF 1731	5.5 (h) x .5 (w)	60s per .5˚	364	6.5

https://doi.org/10.7183/2326-3768.2.2.91 Published online by Cambridge University Press

TABLE 3. The Nine Steps Involved in the CG-1D Neutron Imaging Process.



a batch during a single measurement cycle. Though such batch images are effective for maximizing the number of objects that may be scanned during a user's limited period of beam time, they present methodological challenges for processing the images in the aftermath of collection, since data related to each individual object must be extracted from the batch in the subsequent post-beam time stage of image processing.

Three-dimensional images were also created for one oversized object, a bronze oinochoe vessel that extended vertically beyond the instrument's field of view (Figure 5). To gather three-dimensional data, the oinochoe was imaged separately in two sections, top and bottom, thereby doubling the amount of time required to collect image data during the measurement cycle (Table 2). The two halves of each object were then reunited during post-imaging processing using Photoshop software (Figure 6).

The three-dimensional imaging experiments were invaluable for informing archaeologists and instrument designers alike about the process and limitations of neutron imaging data collection with regard to object size, material, planning, and use of beam time. They also clarified the length of time, computer resources, and technical expertise required for the post-processing and interpretation of images.

IMAGING RESULTS AND INTERPRETATION

Two objects, both imaged in two and three dimensions, offer brief illustrations of how the ORNL neutron imaging techniques are developing alongside archaeological research questions and interpretations.

Earring

A small, heavily corroded circular object (diameter 3 cm), excavated from the Great Temple at Petra, Jordan, was initially believed to be a utilitarian object. Two-dimensional radiography revealed the existence of a delicate, semicircular, metallic object beneath the exterior corrosion layer. Although the object's exact composition remains unknown, the color and characteristics of the thick corrosion layer encasing it initially suggested that it is cupreous. X-ray fluorescence data gathered at ORNL over a year after the initial imaging experiment (once the object cooled and was safe to handle) confirmed that the original object is primarily bronze. The object's circular size and form before imaging appeared similar to a broad range of utilitarian and ornamental items, including horse tack, furniture fittings, and jewelry. Imaging in two and three dimensions produced visual information revealing that the object under the corrosion

https://doi.org/10.7183/2326-3768.2.2.91 Published online by Cambridge University Press

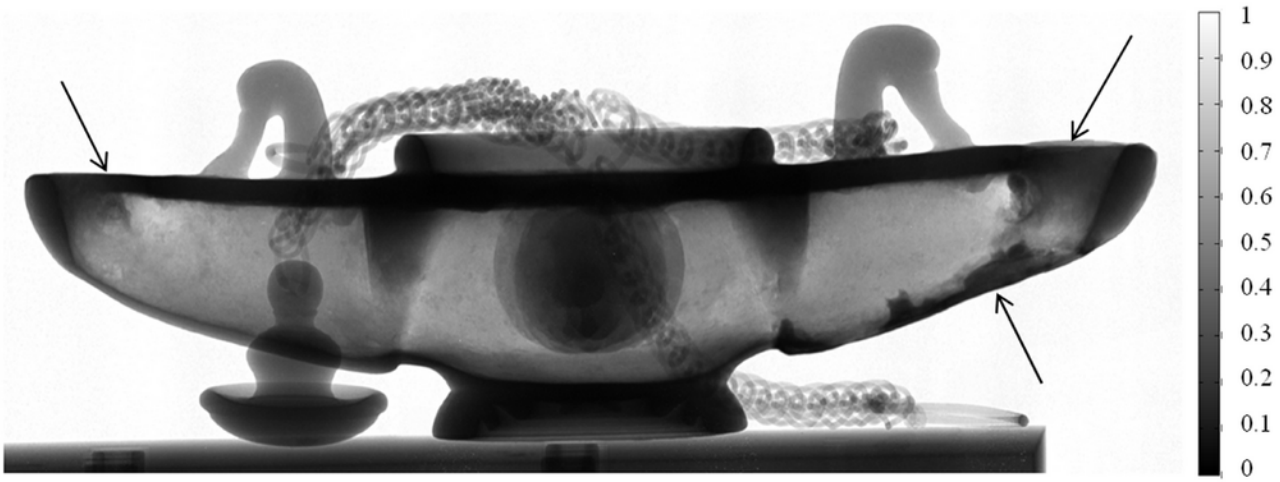


FIGURE 3. Two-dimensional photomosaic neutron radiograph of a Roman-period bronze oil lamp showing interior residue near the lamp openings, as well as evidence of repair to the underside of the right-hand arm. The transmission scale is displayed from 0 to 1 on the right side, where 0 indicates 0% neutron transmission and 1 indicates 100% neutron transmission. The arrow pointing to the bottom of the right arm indicates the repair region. The arrows pointing toward the top of the vessel indicate residue accumulation. (Boscoreale, Italy, JIAAW, LC-025).

layer was most likely an earring. Archaeologically, this earring is significant as one of the few Roman-period personal adornment artifacts recovered from the Great Temple excavations at Petra (Joukowsky 1998:305–306).

Three-dimensional tomography (i.e., neutron CT) produced cross-sectioned slices through the earring. Images document the extent to which the earring's exterior is encased in a thick layer of corrosion (itself containing much internal variation) (Fig-



FIGURE 4. Small metal objects are fit within an area that matches the CG-1D field of view for batch three-dimensional imaging in the same cycle. From left to right: an iron nail from the 18th-century ironworking site at Greene Farm, RI; a brass straight pin from the 17th-century Old House site at Greene Farm; a Roman-period copper alloy spike from the Great Temple excavations at Petra, Jordan; and a 17th-century brass clothing buckle from the Old House site at Greene Farm (Greene Farm objects loaned from Wayne State University; Petra Nail loaned from JIAAW collections).

https://doi.org/10.7183/2326-3768.2.2.91 Published online by Cambridge University Press



FIGURE 5. A Roman-period oinochoe in position for three-dimensional imaging on the rotational platform in front of the CG-1D scintillator. The vessel's height exceeded the instrument's field of view, requiring images to be collected separately for its top and bottom halves. Each imaging cycle took 29.3 hours. (JIAAW, JI-0000-04-0272).



FIGURE 6. Digital reconstruction and volume rendering of the oinochoe in Figure 5 based on the two-dimensional transfer function applied to tomographic image slices.

ure 7). Reconstructed three-dimensional cross-section images of the earring indicate that the metal underneath the corrosion layer is a thin-walled, bronze tubular form (Figure 8). The thin bronze layer rests between the encasing corrosion and an innermost core material. A strong contrast is apparent between the bronze outer wall of the earring and its interior; this variation is likely due to a difference in composition, since a change in density would not typically appear as such a sharp edge. Due to the nature of the neutron beam at CG-1D (i.e., no wavelength discrimination), it is not possible to discern whether the material inside of the earring is corrosion from post-depositional conditions or a different material type that was originally incorporated into the object's core to increase its stability. Future neutron dif-

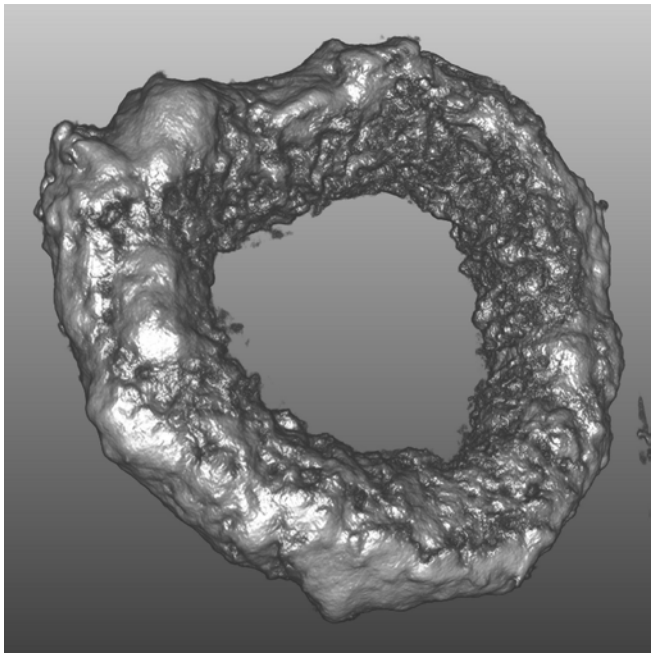


FIGURE 7. Three-dimensional reconstruction and volume rendering of the earring (diameter 3cm) (Great Temple Excavations, Petra, 2001, 79212).

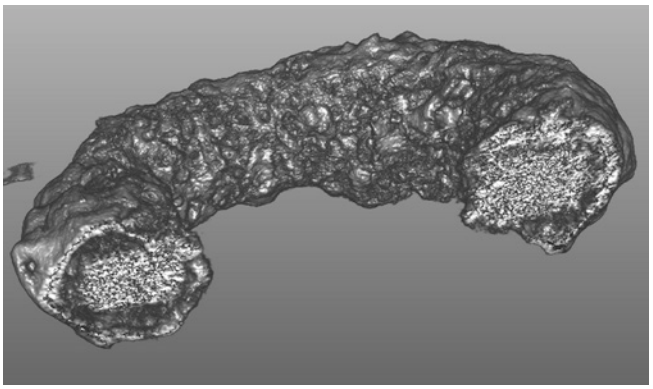


FIGURE 8. A three-dimensional slice through the volume rendering of the earring showing a contrast between the thin metallic layer and the interior region of the object. This contrast is likely due to differences in material composition.

https://doi.org/10.7183/2326-3768.2.2.91 Published online by Cambridge University Press



FIGURE 9. Photograph of dog figurine from from the Wagner Collection of the Joukowsky Institute (JIAAW, JF000-04-0286, 286).

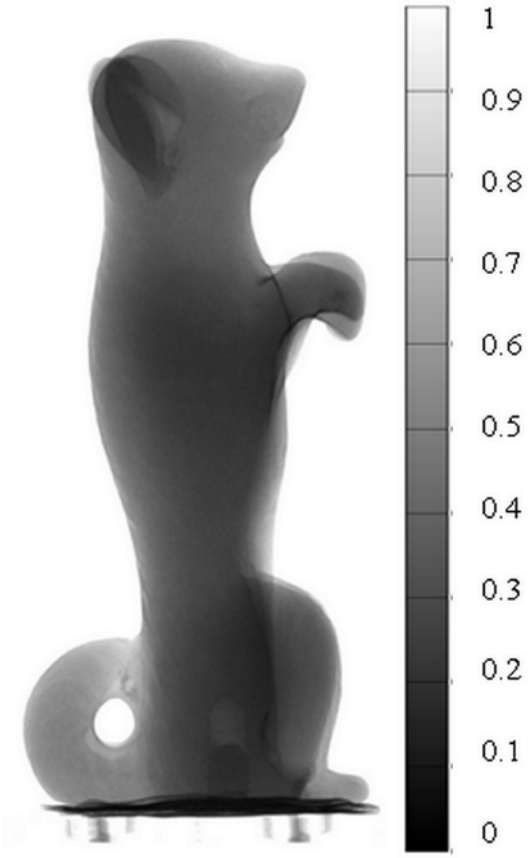


FIGURE 10. Neutron radiograph of the dog figurine. The transmission scale is displayed from 0 to 1 on the neutrograph, where 0 indicates 0% neutron transmission and 1 indicates 100% neutron transmission. A void space is visible at the top of the cylindrical region near the figurine's base (JIAAW, JF000-04-0286, 286).

fraction studies will address compositional questions about the earring and the interior contrast region.

Dog Figurine

The dog figurine is a small cast bronze object dating to the Roman period with incised decorations covering much of the surface, including fur lines and facial details (eyes and snout). The dog stands on its hind legs, has a looped tail, and is missing its left hind paw (Figure 9). Due to the absence of surface corrosion, it was possible to determine from visual inspection that the dog form of the figurine was manufactured from cast techniques (i.e., lost wax).

As reported in Ryzewski et al. (2013), new information about the figurine's manufacture and structural life history were observed during the first two- and three-dimensional imaging experiments conducted on it in 2011. Two-dimensional images first revealed the presence of a cylindrical core region in the interior of the figurine. Processed tomographic images then confirmed the material variability between this region and the remainder of the figurine (Figure 10). These features are visible in a fly-through video of the figurine, produced from its tomographic slices, that transports the viewer from the exterior of the object through its interior (Supplemental Video 1).

During the collection of the radiographs for the neutron CT imaging, a core region, which extended 1 cm into the figurine, was visible. Based on these radiographs and comparisons with other imaged bronze cast objects (de Beer et al. 2009; Festa et al. 2008), it was suggested that the core material of the figurine might be residual clay from the casting process (Ryzewski et al. 2013). Further analysis of the processed tomographic slices from the initial neutron CT image collection revealed a cylindrical region that consisted of a void space directly above a material with a distinctly different attenuation value than the rest of the dog figurine. During subsequent analysis of the tomographic slices from the vertical orientation of the figurine's cylindrical region, researchers identified a grooved inclusion made of a secondary material. The inclusion appears to be the tip of a modern screw, probably broken off from a mounting brace or display platform (Figure 11).

Interpretations of the dog figurine's interior features developed alongside the increased capabilities of neutron CT software and analytical procedures, which permitted the research team to revisit earlier images and address uncertainties. Further mea-

https://doi.org/10.7183/2326-3768.2.2.91 Published online by Cambridge University Press

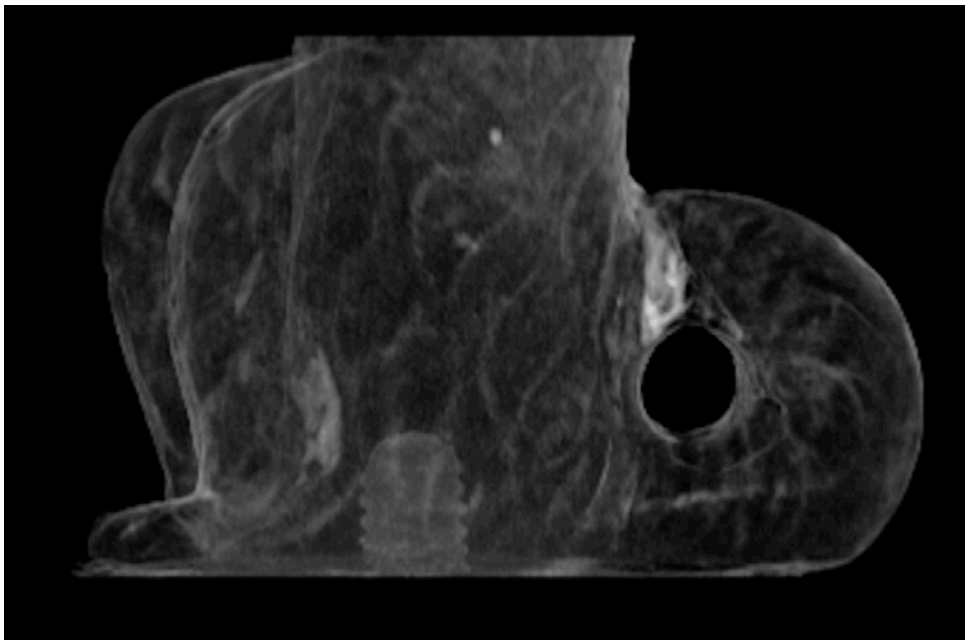


FIGURE 11. A volume rendering of the lower part of the dog figurine, visibly showing the grooves of the broken screw inside.

surements using neutron diffraction are underway to determine compositional differences within the dog figurine. While the CG-1D beamline cannot provide compositional information, its developing counterpart, VENUS, will eventually allow for neutron wavelength-dependent transmission imaging studies (a technique complementary to diffraction studies). The ability to vary neutron wavelength can map Bragg edges (i.e., features that are unique to a specific element) in crystalline structures, thus providing contrast variation and identification of the material.

DISCUSSION

Experiments involving the neutron imaging of 25 archaeological objects with the CG-1D instrument have been productive on two fronts. Most importantly, they have established the methodological procedures and identified the capabilities and constraints involved in imaging archaeological objects with the CG-1D neutron imaging beamline. These procedures include selecting appropriate samples, calculating decay and exposure times, and effectively designing the parameters for three-dimensional image cycles in relation to particular objects' form and material constituents. The experiments have also established and refined the process for analyzing three-dimensional images of archaeological objects by customizing processing software, identifying effective methods for presenting two-dimensional and three-dimensional data, and improving visualizations.

Secondly, the experiments refined neutron imaging methods and capabilities of the CG-1D instrument for the examination of archaeological objects in both two and three dimensions. As image analysis capabilities further develop over the course of the decade, the research team will continue to analyze archaeological objects through the process of reverse engineering. This is a process that requires identifying, understanding, and assembling the three-dimensional neutron imaging data to elucidate information about the materials, techniques, and manufacturing processes of ancient and historical objects, all of which are rarely detailed in past written records.

Ongoing analysis of the archaeological objects imaged with the CG-1D neutron beamline will continue to address current research questions by processing tomographic data, implementing new analytical software capabilities, and refining avenues for future neutron imaging analysis. Such steps involve accessing the energy selective imaging capabilities of the future VENUS beamline. This new capability will allow researchers to enhance material discrimination inside archaeological objects and eventually map changes in an object's material properties and composition across and within its terrain.

Technical and interpretive results for each of the imaged objects to date are to be published as individual case studies in archaeometric, materials science, or physics journals in the upcoming years as the lengthy, multidisciplinary procedure of image processing and analysis is completed by the research team.

CONCLUSION: SUITABILITY OF AND ACCESS TO NEUTRON IMAGING FOR ARCHAEOLOGISTS

Neutron imaging offers archaeologists an unparalleled opportunity to employ a nondestructive technique for gathering two- and three-dimensional data about the properties, structure, performance, and processing of archaeological objects, materials, or residues. Among its advantages over other archaeometric techniques used to examine archaeological materials, neutron imaging produces three-dimensional images of objects, interior and exterior, in which compositional and structural data are present in addition to visual information. Neutron imaging works

https://doi.org/10.7183/2326-3768.2.2.91 Published online by Cambridge University Press

especially well with metals and hydrogen-rich organic materials, and it can map objects of various shapes and sizes. The CG-1D at ORNL is capable of imaging complete objects even when their size exceeds the instrument's 7-x-7-cm^2 field of view.

Before pursuing neutron imaging, it is essential for archaeologists to determine whether the technique will be a productive or possible avenue of analysis for certain material types. For example, the slow radioactive decay rate of some materials, such as silver and zinc, may restrict an object's exposure time to the neutron beam, the quality of resulting image information, and the timely return of objects to their home institution. It is also important that researchers are familiar with complementary archaeometric techniques (e.g., X-ray flouresence, diffraction, and gamma spectroscopy). ORNL research teams often employ these techniques during the preparatory stages of neutron imaging to assist in determining or confirming an object's composition.

Most importantly, archaeologists interested in working with neutron imaging must have expert knowledge about the techniques of manufacture, material properties, and historical context of the artifacts they intend to image. The ability to understand the basic principles of materials science, digital image processing, or analytical computer programs such as MatLab(R)—or at least willingness to learn relevant aspects of these—is useful and can improve the quality of information recovered, as well as the speed with which it is processed.

At ORNL, users propose and conduct imaging experiments with the guidance of Instrument Scientists and other resident researchers with expertise in physics, computer science, and engineering. After undergoing initial instrument training, users operate the CG-1D beamline and DAS software during their allotted period of data collection (i.e., beam time). Although it is expected that users will be capable of operating the imaging instrument and computers independently, at least one resident ORNL scientist regularly consults with users for the duration of their beam time. During the post-imaging stages of research, processing, and analysis, the ORNL scientist works closely with the archeologists to extract meaningful information from the different data sets.

The CG-1D beamline is active during six to seven cycles per year, for 25 days per cycle. Access to the beamline is awarded to archaeologists and other users based upon a competitive, peer-reviewed application process. Applications are available online through the ORNL general user program (http://neutrons.ornl.gov/users/). Successful applicants are allocated a block of beam time that typically ranges from one to several days in length. During beam time, users collect data with the instrument on a continuous, 24-hour basis. There is no cost to users to run the beamline or to process results. All users are required to publish their data in a timely manner.

Over the next few years, as the imaging capability transitions from CG-1D at HFIR to VENUS at the SNS, and as more archaeologists involve neutron imaging in their research, two- and three-dimensional neutron imaging will continue to benefit cross-disciplinary interests, offering archaeologists and materials scientists new perspectives for understanding the manufacturing processes, technologies, and resources involved in the production of archaeological objects.

Acknowledgments

Research at the Oak Ridge National Laboratory's High Flux Isotope Reactor was sponsored by the Scientific User Facilities Division, Office of Basic Energy Sciences, U.S. Department of Energy, which is managed by UT-Battelle, LLC. Funding was also provided by the National Science Foundation, Grant No. DGE0228243. The authors are thankful to: Sophie Voisin of the Biomedical Sciences and Engineering Center at Oak Ridge National Laboratory for her assistance with image processing; Susan E. Alcock, Director of the Joukowsky Institute for Archaeology and the Ancient World at Brown University; and Joel Stone, Curator of the Detroit Historical Museum, for loaning the study objects from their institutional collections. This work was made possible in part by ImageVis3D, which is a software funded by the NIH/NCRR Center for Integrative Biomedical Computing, P41-RR12553-15 and the DOE SciDAC Visualization and Analytics Center for Enabling Technologies, DEFC0206ER.

Supplemental Materials

Supplemental materials are accessible via the SAA member login at http://saa.org/home/tabid/

Supplemental Video 1. Neutron computed tomograph of a Roman-period dog figurine from the Wagner Collection of the Joukowsky Institute.

Data Availability Statement

The data reported in this study were collected at Oak Ridge National Laboratory (ORNL) as part of experiments IPTS-4785, IPTS-6140, and IPTS-7430. Due to security concerns, ORNL does not make their digital data available to the general public via an online archive, database, or website. Data are permanently archived by ORNL on an internal government server. Researchers who wish to request access to the files may contact the current Scientific Data Analysis coordinator at the ORNL DATA Division (http://neutrons.ornl.gov/ndav/; granrothge@ornl.gov). Archaeological artifacts used in this article came from the collections of the Joukowsky Institute for Archaeology and the Ancient World, the Haffenreffer Museum of Anthropology at Brown University, and the Detroit Historical Museum. Specific information on these artifacts is found in Tables 1 and 2. A duplicate of the imaging data set referred to in the article, including metadata and methods, is permanently digitally archived on the Grosscup Museum of Anthropology's server at Wayne State University. The Grosscup Museum is a state repository for archaeological and archival materials, and it is open to the public for research. The data set exists as compressed files and can be shared via file transfer (FTP) upon request. Scholars wishing to access the data should contact the Director of the Grosscup Museum of Anthropology, Dr. Tamara Bray (Tamara.Bray@wayne.edu; +1 (313) 577-2598).

REFERENCES CITED

Anderson, Ian S., Robert L. McGreevy, and Hassina Z. Bilheux (editors)
2009 *Neutron Imaging and Applications: A Reference for the Imaging Community*. New York, Springer.

Andreani, Carla, Giuseppe Gorini, and Thomas Materna
2009 Novel Neutron Imaging Techniques for Cultural Heritage Objects. In *Neutron Imaging and Applications: A Reference for the Imaging*

https://doi.org/10.7183/2326-3768.2.2.91 Published online by Cambridge University Press

Community, edited by Ian S. Anderson, Robert L. McGreevy, and Hassina Z. Bilheux, pp. 229–252, Springer, New York.

Burca, Genoveva, Jon A. James, Winfried Kockelmann, M.E. Fitzpatrick, Shu Yan Zhang, J. Hovind, and Robert van Langh
2011 A New Bridge Technique for Neutron Tomography and Diffraction Measurements. *Nuclear Instruments and Methods in Physics Research Section A: Accelerators, Spectrometers, Detectors and Associated Equipment* 651(1):229–235.

de Beer, Frikkie C., Hazel Botha, Ernst Ferg, Retha Grundlingh, and A. Smith
2009 Archaeology Benefits from Neutron Tomography Investigations in South Africa. *Nuclear Instruments and Methods in Physics Research Section A: Accelerators, Spectrometers, Detectors and Associated Equipment* 605(1):167–170.

Deschler-Erb, Eckhard, Eberhard H. Lehmann, Peter Vontobel, Stefan Hartmann, and L. Pernet
2004 The Complementary Use of Neutrons and X-rays for the Non-Destructive Investigation of Archaeological Objects from Swiss Collections. *Archaeometry*, 46:647– 661.

Dierick, Manuel
2005 Tomographic Imaging Techniques Using Cold and Thermal Neutron Beams. Unpublished Ph.D. dissertation, Department of Physics and Astronomy, Faculty of Sciences, Universiteit Gent.

Festa, Giulia, Paola A. Caroppi, Alessandra Filabozzi, Carla Andreani, M.L. Arancio, Roberto Triolo, Fabrizio Lo Celso, Valerio Benfante, and Silvia Imberti
2008 Composition and Corrosion Phases of Etruscan Bronzes from Villanovan Age. *Measurement Science and Technology* 19(3).

Fiori, Fabrizio, Giuseppe Giunta, Andre Hilger, Nikolay Kardjilov, and Franco Rustichelli
2006 Non-Destructive Characterization of Archaeological Glasses by Neutron Tomography. *Physica B: Physics of Condensed Matter* 385:1206–1208.

Joukowsky, Martha S.
1998 *Petra Great Temple Volume I: Brown University Excavations 1993-1997*. Brown University Petra Exploration Fund, Providence, RI.

Kardjilov, Nickolay, Ingo Manke, Andre Hilger, Scott Williams, Markus Strobl, Robin Woracek, Mirko Boin, Eberhard Lehmann, Dayakar Penumadu, and John Banhart
2012 Neutron Bragg-Edge Mapping of Weld Seams. *International Journal of Materials Research*, 103:151–154.

Kockelmann, Winifred, Gabriel Frei, Eberhard H. Lehmann, Peter Vontobel, and Javier R. Santisteban
2007 Energy-Selective Neutron Transmission Imaging at a Pulsed Source. *Nuclear Instruments and Methods in Physics Research Section A: Accelerators, Spectrometers, Detectors and Associated Equipment* 578(2):421-434.

Lang, Janet, and Andrew Middleton
2005 *Radiography of Cultural Material, 3*. 2nd ed., Elsevier, Burlington.

Lehmann, Eberhard
2006 Scientific Reviews: Using Neutron Imaging Methods for Non- Invasive Investigation of Museum Objects. *Neutron News* 17:22.

Lehmann, Eberhard
2009 Neutron Imaging Methods and Applications. In *Neutron Applications in Earth, Energy, and Environmental Sciences*, edited by L. Liang, R. Rinaldi, H. Schober, pp. 319–350, Springer, New York.

Lehmann, Eberhard, and Helena Pleinert
1998 The New Neutron Radiography Station at the Spallation Source, SINQ, *Insight* 40:192–194.

Lehmann, Eberhard, Eckhard Deschler-Erb, and A. Ford
2010 Neutron Tomography as a Valuable Tool for the Non-Destructive Analysis of Historical Bronze Sculptures. *Archaeometry*, 52:272–285.

Lehmann, Eberhard, Stefan Hartmann, Markus O. Speidel
2010 Investigation of the Content of Ancient Tibetan Metallic Buddha Statues by Means of Neutron Imaging Methods. *Archaeometry*, 52:416–428.

Peetermans, Stevens, Robert van Langh, Eberhard Lehmann, and Arie Pappot
2012 Quantification of the Material Composition of Historical Copper Alloys by Means of Neutron Transmission Measurements. *Journal of Analytical Atomic Spectrometry*, 27:1674–1679.

Penumadu, Dayakar
2009 Material Science and Engineering with Neutron Imaging. In *Neutron Imaging and Applications: A Reference for the Imaging Community*, edited by Ian S. Anderson, Robert L. McGreevy, and Hassina Z. Bilheux, pp. 209–228, Springer, New York.

Prudêncio, Maria Isabel, Marco Antonio Stanojev Pereira, José G. Marques, Maria Isabel Dias, Lurdes Esteves, Christopher I. Burbidge, Maria J. Trindade, and Mestre Beatriz Albuquerque
2012 Neutron Tomography for the Assessment of Consolidant Impregnation Efficiency in Portuguese Glazed Tiles (16th and 18th centuries). *Journal of Archaeological Science* 39:964–969.

Ryzewski, Krysta, Susan N. Herringer, Hassina Z. Bilheux, Lakeisha Walker, Brian W. Sheldon, Jean-Christophe Bilheux, Vincenzo Finocchiaro, and Sophie Voisin
2013 Neutron Imaging of Archaeological Bronzes at the Oak Ridge National Laboratory. *Physics Procedia*, 43:343–351.

Santisteban, Javier R., Lyndon Edwards, Mike E. Fitzpatrick, Axel Steuwer, Philip J.Withers, Mark R. Daymond, Michael W. Johnson, Nigel Rhodes, Erik M. Schooneveld
2002 Strain Imaging by Bragg Edge Neutron Transmission. *Nuclear Instruments and Methods in Physics Research Section A: Accelerators, Spectrometers, Detectors and Associated Equipment* 481(1):765–768.

Schillinger, Burkhard
1996 Three-Dimensional Computer Tomography with Thermal Neutrons at FRM Garching. *Journal of Neutron Research* 4:57–63.

Shatokha, Voldoymyr, Iurii Korobeynikov, Eric Maire, and Jerome Adrien
2009 Application of Three-Dimensional X-ray Tomography to Investigation of Sinter Mixture Granules. *Iron and Steelmaking* 36:416–420.

Tout, R.E., Walter B. Gilboy, and A. J. Clark
1980 The Use of Computerized X-ray Tomography for the Non-Destructive Examination of Archaeological Objects. In *Proceedings of the 18th International Symposium on Archaeometry and Archaeological Prospection, Bonn, 14–17 March 1978*, pp. 608–616. Rheinland-Verlag, Köln.

van Langh, Robert, Jon James, Genoveva Burca, Winfried Kockelmann, Shu Yang Zhang, Eberhard Lehmann, Mirko Estermann, and Arie Pappot
2011 New Insights into Alloy Compositions: Studying Renaissance Bronze Statuettes by Combined Neutron Imaging and Neutron Diffraction Techniques. *Journal of Analytical Atomic Spectrometry* 26:949–958.

van Langh, Robert, Eberhard Lehmann, Stefan Hartmann, Anders Kaestner, and Frits Scholten
2009 The Study of Bronze Statuettes with the Help of Neutron-Imaging Techniques. *Analytical and Bioanalytical Chemistry* 395:1949–1959.

Authors

Krysta Ryzewski ■ Department of Anthropology, Wayne State University, 3054 F/AB, 656 W. Kirby, Detroit, MI 48226 (Krysta.Ryzewski@wayne.edu)

Hassina Z. Bilheux ■ Chemical and Engineering Materials Division, Neutron Sciences Directorate, Oak Ridge National Laboratory, Oak Ridge, TN 37831 (bilheuxhn@ornl.gov)

Susan N. Herringer and **Brian W. Sheldon** ■ School of Engineering, Brown University, Providence, RI 02906 (Susan_Herringer@brown.edu; Brian_Sheldon@brown.edu)

Jean-Christophe Bilheux ■ Neutron Data Analysis and Visualization, Neutron Sciences Directorate, Oak Ridge National Laboratory, Oak Ridge, TN 37831

Lakeisha Walker ■ Research Reactor Division, Neutron Sciences Directorate, Oak Ridge National Laboratory, Oak Ridge, TN 37831 (walkerl@ornl.gov)

https://doi.org/10.7183/2326-3768.2.2.91 Published online by Cambridge University Press